COMMISSIONING THE ECHO-SEEDING EXPERIMENT ECHO-7 AT SLAC*

S. Weathersby, E. Colby, M. Dunning, S. Gilevich, C. Hast, K. Jobe, D. McCormick, J. Nelson, T.O. Raubenheimer, K. Soong, G. Stupakov, Z. Szalata, D. Walz, M. Woodley, D. Xiang
SLAC National Accelerator Laboratory, Menlo Park, CA, 94025, USA
P-L. Pernet, École Polytechnique Fédérale de Lausanne, Lausanne, Switzerland

Abstract

ECHO-7 is a proof-of-principle echo-enabled harmonic generation (EEHG) FEL experiment in the Next Linear Collider Test Accelerator (NLCTA) at SLAC. The experiment is intended to test the EEHG principle at low electron beam energy, 120 MeV, and determine the sensitivities and limitations to understand the expected performance at the higher energy scales and harmonic numbers required for x-ray FELs. In this paper we present the experimental results from the commissioning run of the completed experimental setup which started in April 2010.

INTRODUCTION

The remarkable up-frequency conversion efficiency of the echo-enabled harmonic generation (EEHG) technique [1, 2] has stimulated world-wide interest [3, 4, 5] in using EEHG to achieve fully coherent radiation in the x-ray wavelength from a UV seed laser. Compared with the high-gain harmonic generation (HGHG) [6] technique, EEHG relaxes the requirements on laser power and beam slice energy spread, but requires more challenging control of the phase space correlations as the beam goes through the undulators and chicanes.

The echo-seeding experiment at SLAC (ECHO-7) is a generic EEHG proof-of-principle experiment that uses two different lasers (first laser has a wavelength of 795 nm and the other at 1590 nm) to energy modulate the beam. The first run of the experiment aims to generate the moderate harmonic ($3 \sim 7$) of the second laser, with a staged goal to extend the harmonic number to around 20. Recently the echo signals generated at the 3rd and 4th harmonic of the second laser were observed and clearly differentiated from those generated by the lasers individually [7]. Here we present the results from the commissioning run of the completed experimental setup which started in April 2010.

EXPERIMENT DESCRIPTION

The EEHG beamline is schematically shown in Fig. 1. It consists of 3 chicanes (C0, C1, and C2) and 3 undulators (U1, U2 and U3). The mini-chicane (C0) is used to generate an orbit bump to allow laser injection into the first undulator (U1). The beam is modulated by the 795 nm laser in U1 and after passing through C1 separated energy bands will be generated. The beam is again modulated by 1590 nm laser in the second undulator (U2) and finally the separated energy bands are converted to separated current bands after passage through C2. The density-modulated beam will produce coherent radiation in U3 which is presently tuned to 318 nm. The radiation generated in U3 is reflected by a downstream OTR screen onto a transmission grating spectrometer.

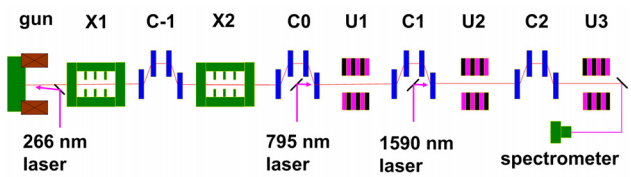

Figure 1: Schematic of the EEHG experiment at SLAC

The experiment required installation of an additional X-band rf structure to boost the existing NLCTA 60 MeV beam to 120 MeV and the fabrication of the three chicanes and undulators. C0 was installed in October 2009 and C1 and C2 were installed in December 2009. A 75 cm long X-band rf structure (X2), installed in December 2009, runs at a gradient of 80 MV/m to boost the beam to 120 MeV. U1 and U2 were installed in February 2010 and the whole beam line was completed in April 2010 with the installation of U3. Now the experiment is under commissioning, with the initial goal of generating the 4th harmonic (ECHO-4) of the second 1590 nm laser. Table 1 lists the operating parameters for the ECHO-4 setup.

Beam-laser interaction is achieved by establishing spatial and temporal overlap. The spatial overlap is achieved by steering the laser to the same position as the beam on the OTR screens upstream and downstream of the undulators. The laser size is about twice that of the electron beam to provide uniform modulation. The position jitter for the electron and lasers are on the order of a few tens of microns which is much smaller than the laser and electron beam size. In order to make the beam temporally overlap with the laser, the undulator radiation and the laser are first sent to a fast photodiode (300 ps rise time). By looking at the signal on a 2.5 GHz oscilloscope we were able to synchronize the laser and electron beam within 30 ps by changing the laser arrival time. More precise timing resolution is achieved by

* Work supported by the US DOE Office of Basic Energy Sciences using the NLCTA facility which is partly supported by US DOE Office of High Energy Physics under Contract No. DE-AC02-76SF00515.

Table 1: ECHO-4 Operating Parameters

Beam energy	120 MeV	
Bunch length	0.5-2 ps	
Normalized emittance	8 mm-mrad	
Bunch charge	20-40 pC	
Laser wavelength in U1	795 nm	
Laser wavelength in U2	1590 nm	seed
Slice energy spread	1 keV	
$N_p \times \lambda_p$ for U1	10×3.3 cm	$K = 1.82$
$N_p \times \lambda_p$ for U2	10×5.5 cm	$K = 2.09$
$N_p \times \lambda_p$ for U3	10×5.5 cm	$K = 1.23$
R_{56} for C1 and C2	1-9 mm	
Peak energy modulation	10-40 keV	
Radiation wavelength	>318 nm	

N_p: number of undulator periods, λ_p: undulator period

using a fast scanning delay stage and measuring the coherent radiation (CR) enhancement that is produced when the beam is energy modulated by each modulator and further bunched by the subsequent dispersive section.

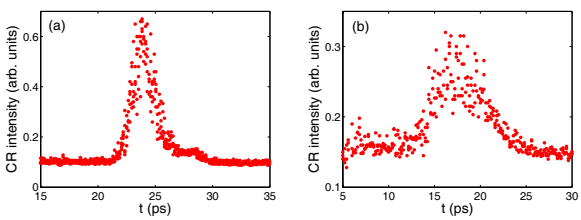

Figure 2: CR intensity vs laser timing. (a) beam is accelerated with on crest phase in X1; (b) beam is accelerated with about 10 degrees off crest in X1.

Two representative results for the CR signal vs the 795 nm laser timing are shown in Fig. 2. The enhancement of the COTR signal is only observed in a short time window in which the laser interacts with the beam. The shape of the time window depends on the electron and the laser distributions. In Fig. 2a the time window is about 1.5 ps and the shape of the CR signal contains a leading peak and a long tail. In Fig. 2b the time window is about 5 ps and the distribution is more Gaussian. This is because in Fig. 2a the beam is accelerated on crest in X1 and after passing through C-1, the head of the beam is compressed and the tail is decompressed, which results in a current distribution that has a leading peak and a long tail. In Fig. 2b the beam is accelerated about 10 degrees off crest so that a positive energy chirp is developed in X1 and the beam is decompressed by about a factor of 4 after C-1. Simulation shows that when the beam is accelerated on crest in X1, due to the nonlinear chirp and the large R_{56} of C-1, the beam will have strong nonlinearities in the longitudinal phase space after C-1 and the slice energy spread varies considerably along the longitudinal direction. A more linear longitudinal phase space and uniform slice energy spread can be achieved by accelerating the beam off crest in X1. For the results shown below the beam is accelerated at about 10 degrees off crest in X1 and is decompressed to about 2.5 ps after C-1.

To detect the ECHO signal an optical spectrometer was set up to measure the radiation generated in U3. The radiation was reflected out of the beam pipe with an OTR through a UV quartz vacuum window onto a transmission grating of 300 lines per millimeter. A CCD camera with a glass lens is positioned at the proper angle to capture the dispersed light. To calibrate the spectrometer, band pass filters at 395 mm and 531 nm, each with 11 nm bandwidth, were remotely inserted while incoherent broad band undulator radiation was present. The detector range was thus determined to be between 350 and 600 nm.

COMMISSIONING RESULTS

Interaction of both lasers together was achieved in May 2010. Direct imaging of the U3 radiation indicated on overwhelming HGHG contribution to the observed coherent enhancement when either or both lasers were interacting [8]. Within the observable bandwidth of the spectrometer both EEHG and HGHG had the same harmonic content. Table 2 lists some of the theoretically predicted harmonics for both EEHG and HGHG in the 350-600 nm range. These were observed for the HGHG case. We note for the EEHG $n = -1, m = 5$ case at 530 nm, there is only 1590 nm harmonic content. To confirm EEHG at 530 nm, it suffices to remove the HGHG contribution. With 1590 nm interaction only, the 530 and 397 nm HGHG signal is observed. By use of a waveplate, the 1590 nm laser is attenuated to the point that the HGHG signals are extinguished. This is shown in Fig. 3a. The 1590 nm laser is then turned off and the 795 nm laser is turned on. Observation reveals the expected 397 nm signal (H2) with no contribution at 530 nm with only the 795 nm laser on. This is shown in Fig. 3b. The attenuated 1590 nm laser is turned back on so that both lasers are interacting. As shown in Fig. 3c, we observe a signal at 530 nm (E0) which we believe to be due to EEHG for $n = -1, m = 5$.

Table 2: Harmonic Content in 350-600 nm

	795 harmonic	1590 harmonic	U3 λ (nm)
HGHG	n=2		397
HGHG		m=3	530
HGHG		m=4	397
EEHG	n=-1	m=5	530
EEHG	n=-1	m=6	397

To distinguish EEHG from HGHG in the observable 350-600 nm bandwidth we make use of a theoretical prediction that spectra will shift differently for EEHG and HGHG in response to a beam energy chirp $h = d\delta/dz$. h is a measure of the change in fractional energy δ along the longitudinal dimension z. For HGHG, the spectra shift in

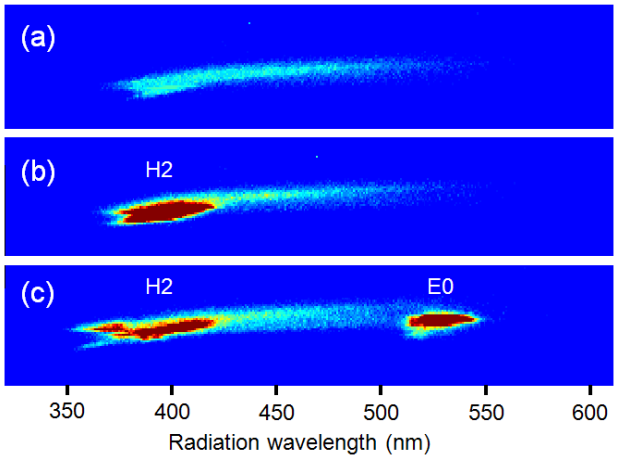

Figure 3: Spectrum of the radiation at the exit of U3: (a) only 1590 nm laser is on and attenuated; (b) only 795 nm laser is on; (c) 795 nm laser and attenuated 1590 nm laser are on.

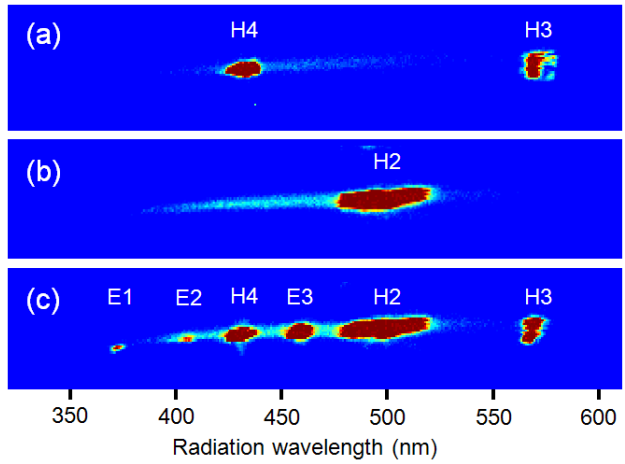

Figure 4: Spectrum of the radiation at the exit of U3 when beam has considerable energy chirp: (a) only 1590 nm laser is on; (b) only 795 nm laser is on; (c) both lasers are on.

terms of the initial wave number k_0, is $k_H = k_0 C$, with a compression factor $C = 1/(1 + hR_{56})$ [9]. In contrast, the EEHG spectra shift in terms of harmonic numbers n, m, initial wave numbers k_1, k_2 and both chicane strengths $R_{56}^{(1)}, R_{56}^{(2)}$ is given by [10]

$$k_E(h) = \frac{nk_1 + (1 + hR_{56}^{(1)})mk_2}{1 + h(R_{56}^{(1)} + R_{56}^{(2)})} \qquad (1)$$

To verify this prediction, we adjusted the phase of X2 to imprint considerable positive energy chirp on the electron beam. As shown in Fig. 4a, due to the energy chirp and the bunch decompression in C2, the 4th harmonic of the 1590 nm laser (H4) shifted from 397.5 nm to about 430 nm, and the 3rd harmonic of the 1590 nm laser (H3) shifted from 530 nm to about 570 nm. Here the 1590 nm laser power is increased to provide an energy modulation amplitude of about 10 keV in the beam so that the harmonic radiation generated by the 1590 nm laser alone can be clearly seen. The radiation is measured downstream of U3, so the compression factor for the modulation generated in U2 is given by $C_{U2} = (1 + hR_{56}^{(1)})/(1 + h(R_{56}^{(1)} + R_{56}^{(2)}))$, where h is the chirp at the entrance to chicane C1. The compression factor is $C_{U2} = 0.9244$ and the chirp is inferred to be $h = 33.4\, m^{-1}$.

The modulation generated in U1 will be decompressed in both C1 and C2, with corresponding compression factor $C_{U1} = 1/(1 + h(R_{56}^{(1)} + R_{56}^{(2)}))$. With this chirp the compression factor for the modulation induced by the 795 nm laser is found to be $C_{U1} = 0.7937$. Accordingly, the wavelength for the 2nd harmonic of the 795 nm laser (H2) should shift from 397.5 nm to 501 nm and was measured at about 499 nm, well within experimental resolution (Fig. 4b).

When both lasers are turned on, 3 additional echo signals with different wavelengths E1, E2 and E3 are observed

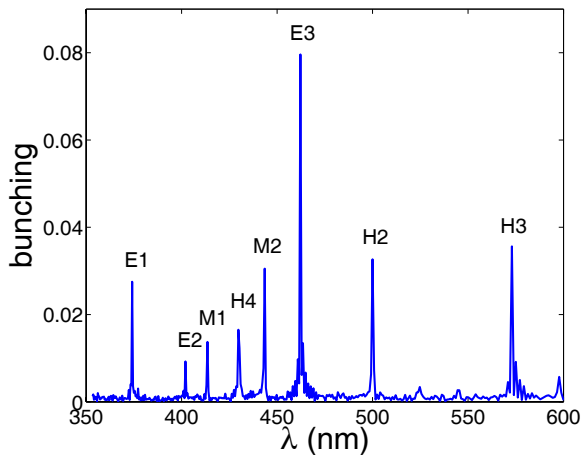

Figure 5: Bunching at various wavelengths from simulation.

(Fig. 4c). The simulated bunching factors for various wavelengths with this chirp are shown in Fig. 5. The beam typically has a slice energy spread of about 1 keV and was decompressed by about a factor of 4 in chicane C-1. Consequently, a slice energy spread of 0.25 keV is assumed in the simulation. The energy modulation amplitudes in U1 and U2 are assumed to be 21 and 10 keV, which is consistent with the experimental values. With these specific parameters, simulation predicts that enhanced coherent radiation at 8 wavelengths may be generated in our experiment.

Analysis shows that the echo signal E1 in Fig. 4 and Fig. 5 is generated with the set $n = -5, m = 4$. It follows from Eq. 1 for the given chirp the wavelength of E1 should shift from 397.5 nm to 374 nm. Experimentally E1 was found shifted to about 373 nm. Similarly the echo signal E2 is found to be generated with the set $n = -1, m = 6$. The wavelength of E2 should shift from 397.5 nm to 402 nm and was measured at 405 nm. E3 is generated with

the set $n = 1, m = 2$. The wavelength of E3 should shift from 530 nm to 462 nm and was measured at about 458 nm. Considering the resolution of the spectromter and some uncertainties of the beam chirp, the experimental results are in good agreement with the EEHG theory.

It should be pointed out, however, that the simulated signals M1 (414 nm) and M2 (444 nm) are missing in our experiment. From simulation we found that the strength of the spectral lines are sensitive functions of modulation amplitudes, which are not well known in the experiment; this may account for the discrepancy. Nevertheless, all the observed spectral lines in the experiment can be well explained with the EEHG theory.

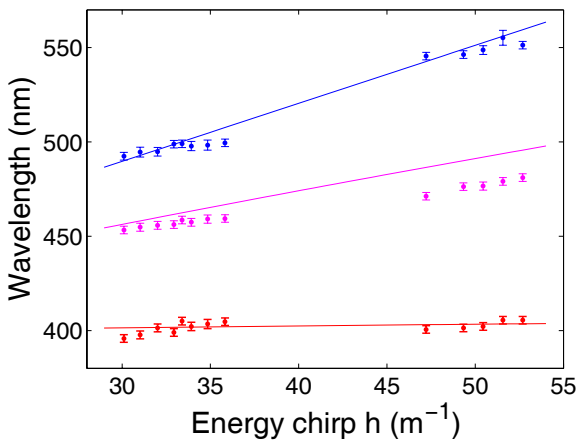

Figure 6: Radiation wavelength vs beam energy chirp for the echo signal E2 (red), E3 (magenta) and that from the 795 nm laser alone H2 (blue). Straight lines are prediction from HGHG and EEHG theory (Eq. 1).

To further benchmark the EEHG theory, the beam energy chirp is varied and the wavelengths of the harmonic radiation for E2, E3, H2 and H4 are measured and shown in Fig. 6 (the E1 signal, being close to the cut-off wavelength of the spectrometer, was not observed in every shot, and is not included in Fig. 6). The chirp factor is inferred from the wavelength shift of H4. The blue dots are the measured wavelength for the 2nd harmonic of the 795 nm laser (H2) and the blue line is the theoretical prediction. The red and magenta dots are the measured wavelength for the echo signal E2 and E3, and the red and magenta lines are the prediction in Eq. 1. The experimental results are in good agreement with the theory. The results confirm that the harmonic radiation wavelength generated by a single laser scales as the compression factor and the sensitivity of the echo signal to the beam chirp depends on n and m. In seeded FELs, the beam energy chirp may be varied to allow fine tunability in the output radiation spectrum.

It is worth mentioning that echo signals at even shorter wavelength could be generated in this experiment setup as well, however, the current diagnostics limit the measurement to optical wavelengths because the transmission of the spectrometer lens drops rapidly below 380 nm. Currently the spectrometer is being upgraded with a UV grade lens to explore the EEHG technique in the shorter wavelength range where the HGHG intensities should diminish.

CONCLUSIONS

We presented initial experimental results from the commissioning efforts for the echo seeding experiment ECHO-7 at SLAC. These results clearly demonstrate that new harmonics were generated from interaction of both lasers with the beam. These new harmonics appear at the expected wavelengths and shift with applied beam energy chirp as predicted by EEHG theory. The good agreement between the EEHG theory and our experimental results confirms the physics behind this technique and paves the way for applying the EEHG technique to future seeded x-ray FELs.

ACKNOWLEDGEMENTS

We thank C. Adolphsen, K. Bane, J. Byrd, A. Chao, J. Corlett, J. Cruz, Y. Ding, P. Emma, W. Fawley, J. Frederico, J. Frisch, G. Hays, Z. Huang, C. Hudspeth, H. Loos, H.-D. Nuhn, G. Penn, S. Prestemon, J. Qiang, M. Racine, R. Schlueter, M. Venturini, W. Wan, F. Wang, X.-J. Wang, W. White, J. Wu and A. Zholents for helpful discussions, comments and commissioning assistance. This work was supported by the US DOE Office of Basic Energy Sciences using the NLCTA facility which is partly supported by US DOE Office of High Energy Physics under Contract No. DE-AC02-76SF00515.

REFERENCES

[1] G. Stupakov, Phys. Rev. Lett, 102 (2009) 074801.

[2] D. Xiang and G. Stupakov, Phys. Rev. ST-AB, 12 (2009) 030702.

[3] D. Xiang and G. Stupakov, "'Coherent soft x-ray generation in the water window with the EEHG scheme"', Proceedings of PAC09; see also SLAC-PUB-13645 (2009).

[4] E. Allaria, G. De Ninno and D. Xiang, "'Feasibility studies for single stage echo-enabled harmonic in FERMI FEL-2"', Proceedings of FEL09.

[5] S. Reiche et al., "'Seeding option for the soft -xray beamline of Swiss FEL"', Proceedings of FEL09.

[6] L.H. Yu, Phys. Rev. A, 44 (1991) 5178.

[7] D. Xiang *et al.*, *First demonstration of the echo-enabled harmonic generation technique for short-wavelength seeded free electron lasers*, to be published in Phys. Rev. Lett; see also SLAC-PUB-14199, (2010).

[8] D. Xiang et al., "Preliminary results of the echo seeding experiment at SLAC", Proceedings of IPAC10.

[9] T. Shaftan and L.-H. Yu, Phys. Rev. E 71, 046501 (2005).

[10] Z. Huang *et al.*, in *Proceedings of FEL 09* (Liverpool, 2009), p.127.